International Journal of Remote Sensing

ISSN: 0143-1161 (Print) 1366-5901 (Online) Journal homepage: https://www.tandfonline.com/loi/tres20

Evaluation and inter-comparison of high-resolution multi-satellite rainfall products over India for the southwest monsoon period

M. Venkatarami Reddy, Ashis K. Mitra, Imranali M. Momin, Ashim K. Mitra & D. S. Pai

To cite this article: M. Venkatarami Reddy, Ashis K. Mitra, Imranali M. Momin, Ashim K. Mitra & D. S. Pai (2019) Evaluation and inter-comparison of high-resolution multi-satellite rainfall products over India for the southwest monsoon period, International Journal of Remote Sensing, 40:12, 4577-4603, DOI: 10.1080/01431161.2019.1569786

To link to this article: https://doi.org/10.1080/01431161.2019.1569786

Published online: 03 Feb 2019.

Submit your article to this journal

Article views: 285

View related articles

View Crossmark data

Citing articles: 1 View citing articles

Full Terms & Conditions of access and use can be found at
https://www.tandfonline.com/action/journalInformation?journalCode=tres20

INTERNATIONAL JOURNAL OF REMOTE SENSING
2019, VOL. 40, NO. 12, 4577–4603
https://doi.org/10.1080/01431161.2019.1569786

Taylor & Francis
Taylor & Francis Group

Check for updates

Evaluation and inter-comparison of high-resolution multi-satellite rainfall products over India for the southwest monsoon period

M. Venkatarami Reddy[a], Ashis K. Mitra[a], Imranali M. Momin[a], Ashim K. Mitra[b] and D. S. Pai[c]

[a]National Centre for Medium Range Weather Forecasting, Earth System Science Organization, Ministry of Earth Sciences, Noida, India; [b]National Satellite Meteorological Center, India Meteorological Department, New Delhi, India; [c]National Climate Centre, India Meteorological Department, Pune, India

ABSTRACT

Rainfall is one of the key drivers of the global hydrological cycle and has large socio-economic impacts. Tropical rainfall accounts for two-thirds of the global rainfall and is primarily associated with the monsoon. Multi-satellite rainfall products provide rainfall with high temporal and spatial resolutions; however, they exhibit regional and seasonal biases. Evaluation of these products against ground-based observations can improve the accuracy of the estimated rainfall. With the launch of the Global Precipitation Measurement (GPM) Core Observatory, two advanced high-resolution multi-satellite precipitation products namely; Integrated Multi-satellite Retrievals for GPM (IMERG) and Global Satellite Mapping of Precipitation (GSMaP) are released. In the present study the spatial and temporal structures of rainfall in near real time and research versions of IMERG-V4 (near real-time (NRT) & Final (FNL)), GSMaP-V6 (NRT & moving vector with Kalman filter (MVK)), INSAT3D (Indian National Satellite System (INSAT) Multispectral Rainfall Algorithm (IMR) & Hydro-Estimator method (HEM)) and Indian Meteorological Department (IMD) – National Centre for Medium Range Weather Forecasting (NCMRWF) Merged product have been evaluated against gridded gauge-based IMD rainfall data on daily, monthly and seasonal scales. All the datasets show noticeable bias in producing rainfall over orographic regions (i.e. Western Ghats and foothills of Himalayas) and North-East India, though there exists significant difference among the satellite measurements. Different skill scores are computed for GSMaP, IMERG and INSAT3D data products to evaluate the performance of these satellite estimates. However in terms of biases IMD-NCMRWF Merged, GSMaP (NRT & MVK) and IMERG (NRT & FNL) underestimates rainfall (about 11%, 17%, 23%, 18% and 3%, respectively) and INSAT3D (IMR & HEM) overestimates (about 49% and 33%, respectively), for the India region as a whole. In a similar way, HEM product shows 15% better performance than IMR product in INSAT3D category. However, both NRT and MVK products of GSMaP show similar variations compared to observe rainfall. Overall IMD–NCMRWF merged and IMERG-FNL data products show better agreement with the gauge-based IMD data compared to GSMaP. The GPM-based products (IMERG and GSMaP) estimate rainfall much better than INSAT3D estimation.

ARTICLE HISTORY
Received 1 April 2018
Accepted 15 October 2018

CONTACT M. Venkatarami Reddy reddyyvu@gmail.com National Centre for Medium Range Weather Forecasting, Earth System Science Organization, Ministry of Earth Sciences, Noida, UP, India

© 2019 Informa UK Limited, trading as Taylor & Francis Group

1. Introduction

Precipitation plays an important role in the global energy and hydrological cycle. Tropical rainfall accounts for about two-thirds of the global rainfall and has large socio-economic impacts. Continuous monitoring of rainfall is essential for the prediction of severe weather, climatological studies of droughts, to reduce the regional damage caused by extreme weather events such as floods and cyclones (Turner and Annamalai 2012; Wang et al. 2012; Webster 2013) and for agricultural applications. Further, high-quality monsoon rainfall estimates are a possible source of information for monsoon modelling and verification of numerical model outputs. Therefore, it is essential to have realistic daily and monthly rainfall datasets over the Indian region, to understand the monsoon rainfall and its variability in a better way. Rainfall data set is made from the rain gauges and ground-based radars (Arkin and Xie 1994; Murali Krishna et al. 2017). However, rain gauges are unevenly distributed and are limited in space (Xie and Arkin 1995). In other hand, the availability of radars is limited with ranges up to around 150 km or less. Satellite measurements provide high temporal resolution and near real-time rainfall estimation over a wide area. A number of multi-satellite precipitation products such as Tropical Rainfall Measuring Mission (TRMM) Multi-satellite Precipitation Analysis (TMPA), Precipitation Estimation from Remotely Sensed Information using Artificial Neural Networks (PERSIANN), Climate Prediction Centre Morphing (CMORPH) and GSMaP (Huffman et al. 2010; Joyce and Xie 2011; Kubota et al. 2007) are developed in the last decade with high spatial and temporal resolution by combining the precipitation information from multiple sensors (such as, passive microwave (PMW) sensors and infrared (IR) radiometers) and multiple algorithms (Adler and Negri 1988; Arkin, Joyce, and Janowiak 1994; Ferraro et al. 2005; Aonashi et al. 2009).

The Global Precipitation Measurement (GPM) mission was launched in February 2014 to provide next-generation global rain as well as snow observations in near real-time (Hou et al. 2014; Yong et al. 2015). The GPM is a joint mission between the National Aeronautics and Space Administration (NASA) and the Japan Aerospace Exploration Agency (JAXA), providing the next-generation rainfall products (Hou et al. 2008). It carries an advanced 13-channel passive microwave radiometer, namely, GPM Microwave Imager (GMI), paired with a K_a/K_u-band dual-frequency precipitation radar (DPR). The purpose of the DPR is to estimate light as well as extreme precipitation more precisely. Several researchers focused on the evaluation of the IMERG rainfall estimates against ground-based (radar and gauge) and other satellite measurements. Recently, Murali Krishna et al. (2017) evaluated the IMERG rainfall products on diurnal, monthly and seasonal basis over Indian subcontinent using rain gauge, disdrometer and TRMM measurements. They found that the IMERG estimated rainfall is comparable with the rainfall observed from rain gauges and disdrometer in all the time scales than TRMM measurements. The comparison of IMERG and TMPA product reveals that the IMERG exhibits better performance than TMPA, especially at light and heavy precipitation (Chen and Li 2016; Liu 2016; Tang et al. 2016; Sharifi, Steinacker, and Saghafian 2016; Ma et al. 2016; Siuki, Saghafian & Moazami 2017; Wang, Chen, and Wang 2017). Sungmin et al. (2017) reported that the IMERG Final (IMERG-FNL) product is superior to IMERG Early and Late (NRT: near real-time) products over southeast Austria. Several researchers investigated the uncertainties in the IMERG V03 product and revealed that the IMERG V04

performs better than IMERG V03 (Ma et al. 2016; Guo et al. 2016; Gaona et al. 2016; Tan, Petersen, and Tokay 2016; Asong et al. 2017). IMERG V04 is upgraded compared to V03 by employing the 2017 version of the Goddard Profiling Algorithm (GPROF2017v1) and the Advanced Temperature and Moisture Sounder (ATMS) for precipitation estimation. Additional changes include calibrating IR to HQ data, 2BCMB to GPCP V2.3, etc. (Huffman et al. 2017). The present study is focussed on the IMERG V04 products over Indian region for the monsoon period.

The Global Satellite Mapping of Precipitation (GSMaP) is a multi-satellite rainfall product based on blending PMW and IR data. Several researchers validated the GSMaP moving vector with Kalman filter (GSMaP-MVK) product over different locations and revealed that the GSMaP-MVK detects the occurrence of precipitation. However, it generally underestimates the amount of precipitation compared to rain gauges and other satellite measurements (Dinku et al. 2009). Kubota et al. (2009) validated the GSMaP rainfall product using gauge-calibrated ground radar data sets over Japan. They reported that the GSMaP produced the gridded gauge rainfall over most parts of the study regions except over the mountainous and coastal regions. They also found that, in some cases, GSMaP-MVK data still underestimates the rain gauge data. Prakash et al. (2016a) compared the older version of GSMaP products with Indian Meteorological Department (IMD) gauge-based observations over Indian region and found that the GSMaP products show poor performance over the Western Ghats (WG) and over south-east peninsular India.

Recently, Indian Space Research Organisation (ISRO) launched a series of meteorological satellites, Indian National Satellite system (INSAT) 3D to monitor the Earth's surface and environment. INSAT3D carries a multi-spectral Imager (optical radiometer) capable of generating images of the Earth in six wavelength bands. The INSAT3D Imager has 1 km resolution in the visible band for monitoring of mesoscale phenomena and severe local storms. The short-wave infrared (SWIR) and middle infrared (MIR) bands has the resolutions of 1 and 4 km, respectively, enables better land–cloud discrimination and detection of surface features such as snow. The TIR band with 4 km resolution helps in the extraction of sea-surface temperature with far greater accuracy. The Imager generates images of the Earth's disc from a geostationary altitude of 36, 000 km every 26 min and provides information on various parameters, namely, outgoing long-wave radiation, quantitative precipitation estimation, sea-surface temperature, snow cover, cloud motion winds, etc. Mitra et al. (2018) evaluated the INSAT3D rainfall products of Hydro-Estimator Method (HEM), INSAT Multi-spectral rainfall (IMR) and Quantitative Precipitation Estimation (QPE) for the analysis of heavy rainfall episodes over the Indian region.

In the present study, an attempt is made to inter-compare the newly launched GPM rainfall products (V4 of IMERG-NRT & FNL), V6 of GSMaP-NRT& MVK), INSAT3D rainfall products (IMR & HEM) and IMD – National Centre for Medium Range Weather Forecasting (NCMRWF) merged rainfall products. Also, an assessment is carried out to find out any differences and improvements, with cross-evaluation against the IMD gridded gauge-based data sets over the Indian region during the summer monsoon season 2016 (JJAS-2016). To quantify the performance of the satellite measurements, several statistical skill scores are computed and inter-compared.

2. Data and methodology

2.1. *IMD gauge-based rainfall data*

The daily gridded gauge-based rainfall data from the India Meteorological Department (IMD) are used to evaluate GPM and INSAT3D-based satellite estimates for the Indian monsoon period June–September 2016 (JJAS 2016). These surface rain gauge (SRG) based gridded rainfall data are available at a spatial resolution of 0.25° latitude/longitude since January 1901 (Pai et al. 2014, 2015). This data set consists of daily rainfall observations collected from about 3500 quality checked rain gauges situated in different locations over India. The distribution of these rain gauges is adequate over Indian region, except some small regions of Jammu and Kashmir (J&K) and extreme north-west parts of India. This rainfall dataset represents more realistically the orographic rainfall compared to other rainfall data sets measured by the rain gauges (Pai et al. 2014, 2015).

2.2. *IMD–NCMRWF merged data*

IMD–NCMRWF merged (Merged) gridded rainfall data used in the present study is based on a successive correction method (Mitra et al. 2003). The first guess rainfall information is obtained from satellite estimates over land and ocean. Mitra et al. (2009) used the TMPA estimates as a first-guess for the merged satellite-gauge algorithm. The successive correction method used there is similar to Cressman (1959), which modifies the initial guess (satellite estimates) based on the observations (rain gauge). In their method, the first guess value for each station is obtained by interpolating the satellite measurements. The difference between the observed value and first guess provides the error estimate at the station location. The corrections at each grid point are obtained by using the successive iterative corrections on these error estimates. Mitra et al. (2003, 2009) discussed the details of weights and interpolations for this successive iteration correction. In the present study, GPM-based GSMaP-NRT data available at 0.1° spatial resolution and half hour temporal resolution is upscale and used as the first guess for the NCMRWF daily merged satellite gauge rainfall analysis. This 0.1° spatial resolution data is interpolated to obtain 0.25° resolution data. The daily accumulated rainfall data ending at 0300 UTC is calculated from hourly GSMaP-NRT data for their compatibility with the IMD gauge-based data ending at 0300 UTC.

2.3. *IMERG*

The GPM mission, successor of TRMM is a joint mission between the NASA and the JAXA, providing the next-generation rainfall products (Hou et al. 2008). Integrated Multi-satellite Retrievals for GPM (IMERG) is a multi-satellite precipitation product which is obtained by combining PMW and IR data of GPM constellation satellites. This multi-satellite precipitation product is calibrated by gauge analysis of the Global Precipitation Climatology Centre (GPCC) (Schneider et al. 2008). The IMERG data is available at a spatial resolution of 0.1° and temporal resolution of 30 min. The processing of IMERG includes 1) the CMORPH-KF for quality-weighted time interpolation ('morphing') of PMW estimates following cloud motion vectors (Joyce et al. 2004; Joyce and Xie 2011), 2) the PERSIANN-CCS for retrieving PMW-calibrated IR estimates (Sorooshian et al.

2000; Hong et al. 2004), and, 3) the TMPA for inter-satellite calibration and monthly gauge adjustment (Huffman et al. 2007). The details of data and algorithm description can be found in Huffman et al. (2015).

In the present study, IMERG version 4 data products are evaluated against the IMD gridded rainfall data. The level 3 IMERG products provide rainfall and snowfall at 0.1° spatial and half hour temporal resolutions. The algorithm of IMERG system runs twice in near real-time, 'Early' and 'Late' multi-satellite products. The Late multi-satellite retrievals (IMERG-NRT) provide data at around 18 h after the observation time. Once after the monthly gauge analysis is received, the final product is run to create the final (IMERG-FNL) data around 3 months after the observation time. However, the IMERG-E and IMERG-NRT runs use only part of the IMERG processing steps. For example, the instantaneous PMW rainfall estimates are propagated only forward in time by the morphing scheme in the IMERG-E run, whereas both forward and backward morphing schemes are used in IMERG-NRT and IMERG-FNL runs. Hence, IMERG-NRT and IMERG-FNL runs are likely to be better describing changes in the intensity and shape of rainfall features compared to IMERG-E.

2.4. *GSMaP*

GSMaP is a multi-satellite precipitation estimates initiated by the Core Research for Evolutional Science and Technology (CREST) of the Japan Science and Technology Agency (JST) during 2002–2007 and has been promoted by the JAXA Precipitation Measuring Mission (PMM) science team since 2007 to produce a global precipitation product with high temporal and spatial resolution (Ushio et al. 2009). GSMaP uses both microwave and IR satellite observations at high temporal and spatial resolution (Kubota et al. 2007). The Climate Prediction Center (CPC) daily gauge analyses are used for bias-correction in the GSMaP estimates. It provides rainfall estimates in both near real-time (GSMaP-NRT) and delayed mode (GSMaP-MVK). Both the datasets use Kalman filter model to integrate the passive microwave and IR satellite datasets. The versions 6 of GSMaP precipitation estimates are available at 0.1° spatial resolution and 1 hr temporal resolution from 60°N to 60°S.

2.5. *INSAT3D*

INSAT3D carries a multi-spectral Imager (optical radiometer) capable of generating images of the Earth in six wavelength bands, namely visible (Vis), SWIR, MIR, water vapour (WV) and two bands in the thermal infrared (TIR1 and TIR2) region. The ground resolution at the sub-satellite point is nominally 1 km × 1 km for visible and SWIR bands, 4 km × 4 km for one MIR and both TIR bands and 8 km × 8 km for WV band. The INSAT3D estimates the rainfall based on three methodologies: (i) Geostationary Operational Environmental Satellite (GOES) Precipitation Index (GPI), (ii) INSAT Multispectral Rainfall Algorithm (IMR) and (iii) Hydro-Estimator method (HEM). In the present study, the rainfall is estimated using IMR and HEM method are analysed. IMR uses multiple regression based empirical relationship to estimate rainfall from Infra-Red channels. The IMR approach can be used to optimize the identification of raining clouds and to identify the location of rain/rain rate quantitatively (Ba and Gruber 2001). The HEM is operationally implemented to estimate rainfall with high temporal and spatial resolution from INSAT3D measurements. HEM method uses TIR measurements

at 10.7 μm with National Centers for Environmental Prediction (NCEP) Global Forecasting System (GFS), and an atmospheric thermodynamic model derives environmental parameters along with a surface topography model. The HEM method is remodelled (Varma and Gairola 2015; Mitra et al. 2018) and is used for INSAT3D satellite for the present study.

2.6. Methodology

The GSMaP data is re-sampled to 0.25°×0.25° spatial grids using the linear averaging method to compare with the IMD gauge-based data. Further, the IMERG and INSAT3D data are also re-sampled to 0.25° spatial resolution to facilitate comparison. All the nearest grid points (0.1°) of IMERG, INSAT3D and GSMaP around a 0.25° grid are considered for the linear averaging. Further, the SRG-based daily rainfall data set accumulates rainfall ending at 0300 UTC whereas the IMERG and GSMaP accumulates daily rainfall ending at 0000 UTC. For this purpose, the rainfall accumulations are calculated ending at 0300 UTC from GSMaP and IMERG datasets. There are 122 data points (17 weeks *per* year) at each grid within India for comparison for the said monsoon period of 2016. To assess the accuracy of the Merged, GSMaP, IMERG and INSAT3D data, various popular skill metrics such as Bias, Percentage Bias (P Bias), root-mean square error (RMSE), Percentage RMSE (P RMSE), correlation coefficient (r), estimated the following Equations:

$$\text{Bias} = \frac{\sum_{i=1}^{N}(S_i - G_i)}{N} \tag{1}$$

$$\text{P Bias} = \frac{\sum_{i=1}^{N}(S_i - G_i)}{\bar{G}} \times 100 \tag{2}$$

$$\text{RMSE} = \sqrt{\frac{1}{N}\sum_{i=1}^{N}(S_i - G_i)^2} \tag{3}$$

$$\text{PRMSE} = \frac{\sqrt{\frac{1}{N}\sum_{i=1}^{N}(S_i - G_i)^2}}{\bar{G}} \times 100 \tag{4}$$

$$r = \frac{\sum_{i=1}^{N}(S_i - \bar{S})\,(G_i - \bar{G})}{\sqrt{\sum_{i=1}^{N}(S_i - \bar{S})^2}\sqrt{\sum_{i=1}^{N}(S_i - \bar{G})^2}} \tag{5}$$

Where G = IMD gauge-based data, $\bar{G}$= average of gauge-based data, S = Satellite data (i.e. Merged, GSMaP, IMERG and INSAT3D), $\bar{S}$= average of Satellite data and N = number of data pairs.

In addition, probability of detection (POD), false alarm ratio (FAR), frequency bias index (FBI) and threat score (TS)/critical success index (CSI) are computed to examine the capability of each satellite measurement. These standard skill metrics are computed on the basis of a 2 × 2 rain contingency table (Table 1) (Wilks 2006; Hogan et al. 2010). The rainfall rate of 1 mm day^{-1} is considered as a threshold value for this contingency table. POD provides the rain events successfully identified by the satellite measurements, FAR is a measure of tendency of satellite product to detect rain when there was no rain is observed. The frequency of detection of rainfall by the satellite measurements is

Table 1. A contingency table and definitions for comparing IMD gauge-based and satellite estimates.

	Gauge rain	Gauge no-rain
Estimated rain	Hits (*a*)	False alarms (*b*)
Estimated no-rain	Misses (*c*)	Correct rejects (*d*)
Probability of detection (POD)	$POD = \frac{a}{a+c}$	
False alarm ratio (FAR)	$FAR = \frac{b}{a+b}$	
Frequency bias index (FBI)	$FBI = \frac{a+b}{a+c}$	
Critical success index (CSI)	$CSI = \frac{a}{a+b+c}$	

provided by FBI and the portion of rainfall events that are correctly detected by the satellite measurements is given by CSI. For a perfect satellite-based estimate, the values of POD, FAR, FBI and CSI should be 1, 0, 1 and 1, respectively.

3. Results and discussions

3.1. *Spatially inter-comparison of high-resolution products over India*

In this section, the spatial distributions of mean monsoon rainfall and various skill metrics against IMD gridded gauge-based data are presented for the period 2016 over India. Figure 1 shows the mean seasonal (JJAS) rainfall observed by IMD, Merged, and

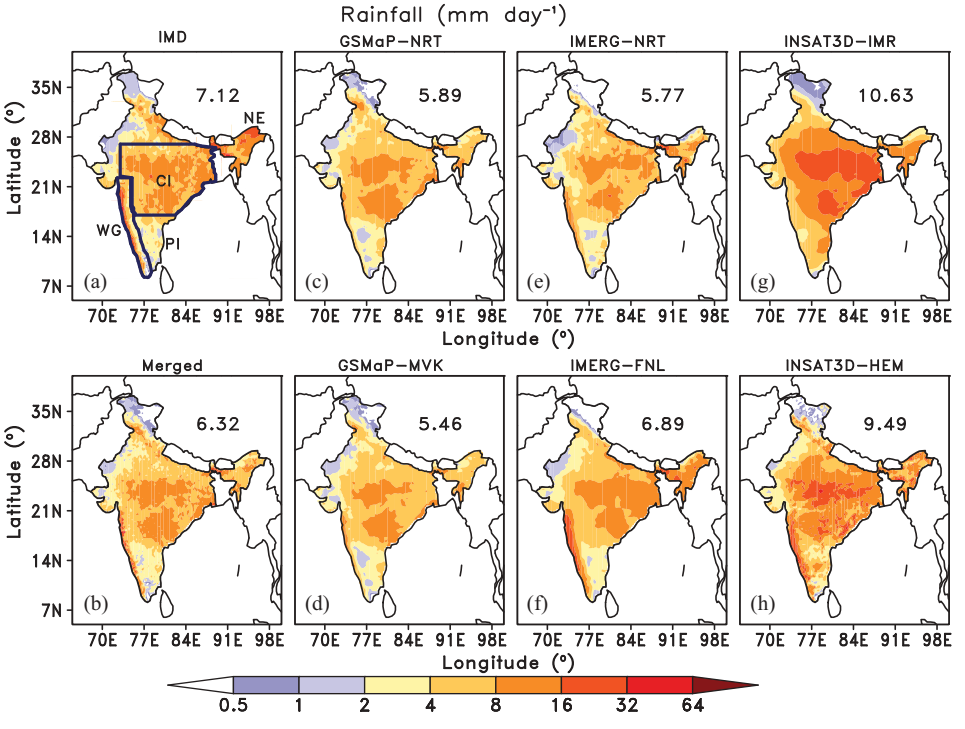

Figure 1. Spatial distributions of mean daily rainfall (mm day^{-1}) during the southwest monsoon (JJAS 2016) over India from (a) IMD, (b) Merged, (c) GSMaP-NRT, (d) GSMaP-MVK, (e) IMERG-NRT, (f) IMERG-FNL, (g) INSAT3D-IMR and (h) INSAT3D-HEM products. Mean rainfall values averaged over India are given in the parentheses.

GSMaP-NRT, GSMaP-MVK, IMERG-NRT, IMERG-FNL, INSAT3D-IMR and INSAT3D-HEM products. The summer monsoon rainfall shows two maxima (>16 mm day^{-1}): one along the west coast of India (WG) and the other in the north-eastern regions of India due to varied orography and monsoonal flow. Second by, another region of high rainfall is associated with monsoon trough zone as well as foot hills of Himalayas. In general, the north-west India, J&K and southeast peninsular India receives lower rainfall during the summer monsoon season. A sharp west-to-east gradient in rainfall is observed over southern India. The large-scale patterns of the monsoon rainfall such as heavier orographic rainfall along the WG Mountains and in north-east (NE) India, and lower rainfall over the north-west desert region and rain-shadow region of Southeast Peninsular India is qualitatively captured by Merged, GSMaP and IMERG rainfall products.

However, quantitative comparisons reveal some differences among them. Merged rainfall product shows less rainfall over WG (<16 mm day^{-1}), NE regions (<16 mm day^{-1}), foothills of Himalayas (< 8 mm day^{-1}), as well as monsoon trough region. On the other hand, GSMaP-NRT product shows less rainfall (<8 mm day^{-1}) along the WG mountain region, foothills of Himalayas, north-eastern regions and higher amounts (>8 mm day^{-1}) over monsoon trough region and southern peninsular India. This can be observed by negative and positive biases observed in these regions respectively (Figure 2). IMERG-NRT rainfall product shows higher rainfall (>8 mm day^{-1}) over foothills of Himalayas, central Indian eastern parts and southern peninsular India. However, it shows lower

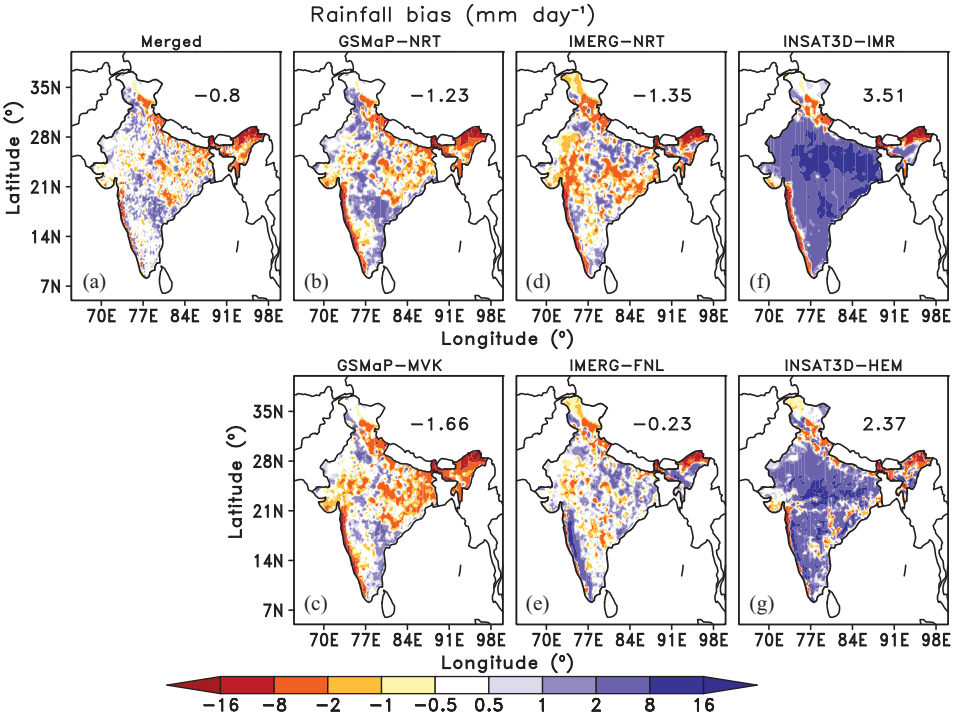

Figure 2. Spatial distributions of mean daily rainfall bias (mm day^{-1}) during the southwest monsoon (JJAS 2016) over India from (a) Merged, (b) GSMaP-NRT, (c) GSMaP-MVK, (d) IMERG-NRT, (e) IMERG-FNL, (f) INSAT3D-IMR and (g) INSAT3D-HEM products with respect to IMD-SRG data. Mean rainfall bias values averaged over India are given in the parentheses.

rainfall (<8 mm day^{-1}) over WG and north-eastern regions. But, IMERG-FNL product shows much improvement over WG, north-eastern regions and foothills of Himalayas compared to IMERG-NRT product. However, the INSAT3D-IMR product shows higher rainfall (>16 mm day^{-1}) over central India and south east peninsular regions, whereas it shows lower rainfall (<mm day^{-1}) over WG, parts of north-eastern regions and foothills of Himalayas. INSAT3D-HEM product shows higher rainfall (>16 mm day^{-1}) over most of the regions (central India). Overall, the Merged product are qualitatively and quantitatively better than IMERG-NRT, GSMaP and INSAT3D products.

The daily average rainfall bias for Merged, GSMaP-NRT, GSMaP-MVK, IMERG-NRT, IMERG-FNL, INSAT3D-IMR, and INSAT3D-HEM with respect to the gridded gauge-based product is shown in Figure 2. Merged rainfall shows better estimation over all the regions except over NE regions of India. It shows a positive bias in most of the regions and negative bias over NE regions. GSMaP-NRT and GSMaP-MVK also shows less bias (<±2 mm day^{-1}) except over WG and NE regions. Both the GSMaP products also show negative bias over WG and NE regions. The INSAT3D products show overestimated and higher biases (>8 mm day^{-1}) compared to all other products. The IMERG-NRT product also shows similar biases. It shows negative bias over NE regions and parts of WG, whereas IMERG-FNL shows positive bias in WG. Overall, IMERG-FNL shows better comparison with less bias over most of the regions compared to other satellite products. The mean daily rainfall (bias) averaged over the whole Indian region for the monsoon season of 2016 from IMD gauge-based, Merged, GSMaP-NRT, GSMaP-MVK, IMERG-NRT, IMERG-FNL, INSAT3D-IMR, and INSAT3D-HEM are 7.12 mm, 6.32 mm (−0.8 mm), 5.89 mm (−1.23 mm), 5.46 mm (−1.66 mm), 5.77 mm (−1.35 mm), 6.89 mm (−0.23 mm), 10.63 mm (3.51 mm) and 9.49 mm (2.37 mm) respectively. This indicates that the Merged, IMERG and GSMaP products underestimated the monsoon rainfall averaged over India whereas INSAT3D products overestimated when compared to gauge-based data set. These results are consistent with the previous studies by Qin et al. (2014) and Prakash et al. (2016) that the GSMaP-NRT product underestimates the rainfall over most parts of India.

Further, the spatial distribution of statistical indices such as RMSE and '*r*' are calculated and the results are now discussed. The spatial distribution of RMSE and '*r*' for Merged, GSMaP-NRT, GSMaP-MVK, IMERG-NRT, IMERG-FNL, INSAT3D-IMR and INSAT3D-HEM products with respect to IMD gauge-based data are presented in Figures 3 and 4. The Merged product shows higher RMSE (>20 mm day^{-1}) over few places of NE region, WG and central India. The IMERG-NRT product shows higher RMSE (>mm day^{-1}) values over WG, foothills of Himalayas, NE and Central India. GSMaP-MVK and GSMaP-NRT shows relatively lower RMSE values compared to IMERG-NRT product. The INSAT3D products show higher RMSE (>24 mm day^{-1}) values compared to all other products. Merged data product shows very less RMSE values compared to other products, however the average value of RMSE over all the grid points is 11.26 mm day^{-1} for Merged data set. The spatial distribution of '*r*' shows that Merged, GSMaP and IMERG products shows better correlation with a magnitude higher than 0.6 over all the regions. The correlation is higher (>0.8) in north-western parts, Central India, and soutern peninsular India compared to other regions. Both the GSMaP and IMERG products show good correlation except the northern and north-eastern parts of the country where the correlation is below 0.4. Among all the data products, Merged product shows better '*r*'

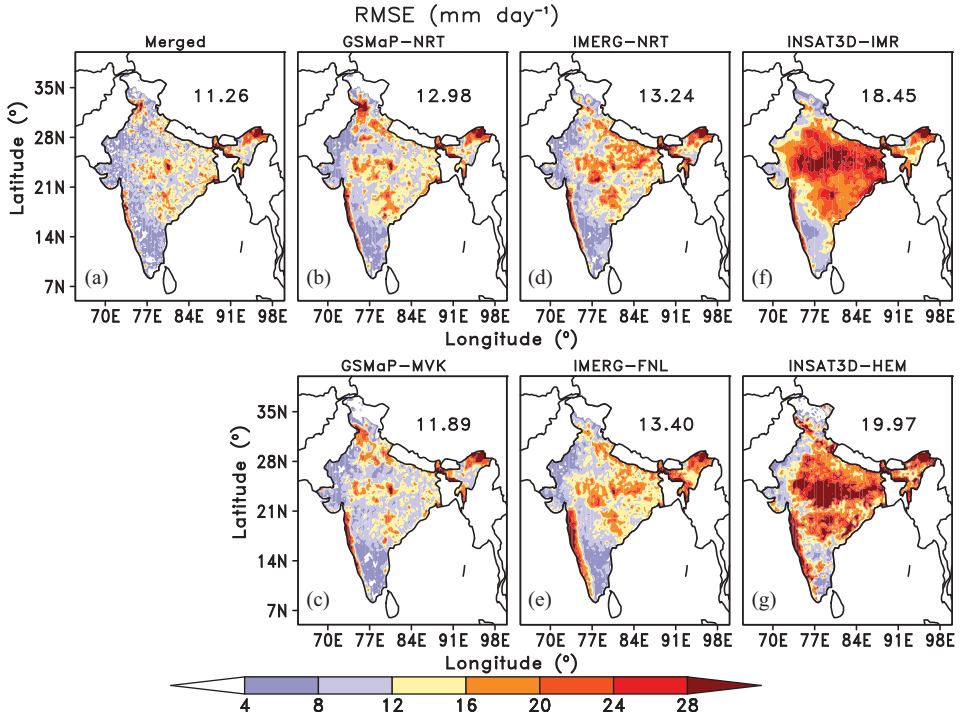

Figure 3. Spatial distributions of RMSE (mm day^{-1}) during the southwest monsoon (JJAS 2016) over India from (a) Merged, (b) GSMaP-NRT, (c) GSMaP-MVK, (d) IMERG-NRT,(e) IMERG-FNL, (f) INSAT3D-IMR and (g) INSAT3D-HEM products with respect to IMD-SRG data. Mean values of RMSE averaged over India are also given in the parentheses.

over most of the regions of India. But the average value of '*r*' over all the grid points for the Merged data set is 0.61 and is 0.56 for IMERG-FNL&GSMaP-MVK data sets.

Figure 5 shows a comparison of averaged daily monsoon (June–September) rainfall at each grid point over India from various products such as Merged, GSMaP-NRT, GSMaP-MVK, IMERG-NRT, IMERG-FNL, INSAT3D-IMR and INSAT3D-HEM with IMD gauge-based data. In this figure, the red dash line indicates the 1:1 line in the comparison. It is clearly observed from this figure that Merged and IMERG-FNL shows higher correlation (r = 0.7) and lower RMSE (3.9 mm day^{-1}). The daily mean rainfall seems to be uniformly distributed about the 1:1 line in Merged data product. The INSAT3D-IMR shows least correlation (r = 0.307) with IMD gridded data set. In GSMaP-NRT and GSMaP-MVK (IMERG-NRT and IMERG-FNL) products, the daily accumulated rainfall does not exceed 20 mm (30 mm). Whereas in Merged and INSAT3D data products, the daily accumulated rainfall exceeds 50 mm. Further, the GSMaP products underestimate the mean monsoon rainfall whereas the INSAT3D products overestimates mean monsoon rainfall over India when compared with the IMD gridded data.

The spatial distributions of POD and FAR are shown in Figures 6 and 7 respectively. All these satellite-based rainfall datasets show higher POD (>0.7) over most parts of India except over J&K. This indicates that all the products are able to capture the rainfall occurrence quite well. However, the GSMaP products show less POD (<0.7) over WG

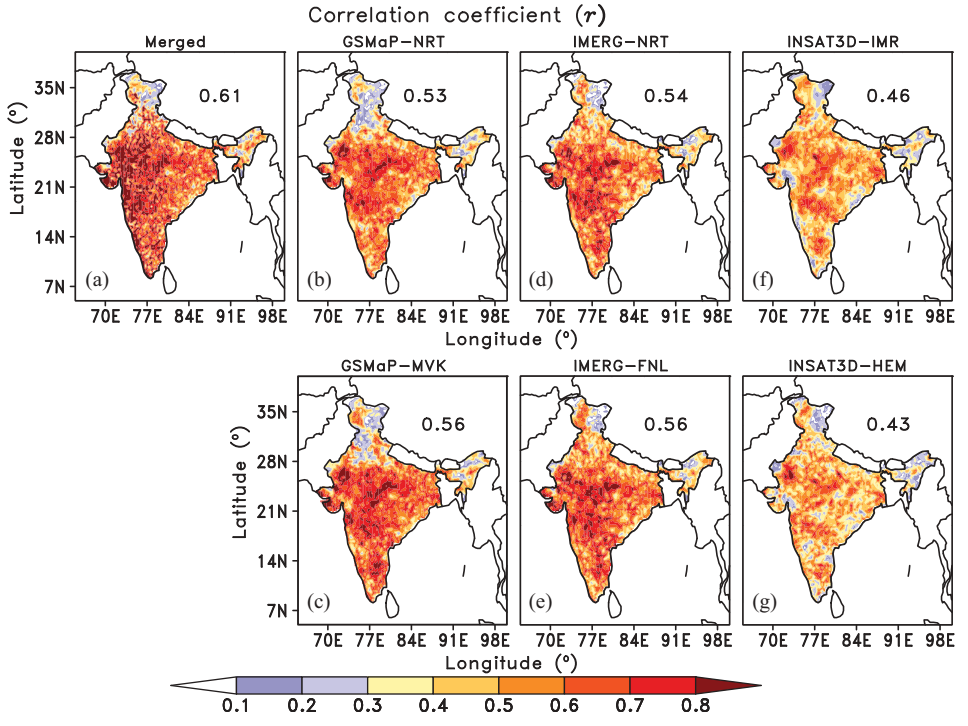

Figure 4. Spatial distributions of Correlation coefficient (r) during the southwest monsoon (JJAS 2016) over India from (a) Merged, (b) GSMaP-NRT, (c) GSMaP-MVK, (d) IMERG-NRT,(e) IMERG-FNL, (f) INSAT3D-IMR and (g) INSAT3D-HEM products with respect to IMD-SRG data. Mean values of Correlation coefficient averaged over India are also given in the parentheses.

region also. Merged, IMERG-NRT, and IMERG-FNL shows higher POD than GSMaP and INSAT3D-HEM data sets. Similar to POD, in other hand the satellite-based data sets show lower FAR over most of the regions. FAR shows higher values over J&K (>0.8), southeast peninsula (>0.8) and north-west (>0.4) parts of India in all the data products, which shows its inability to detect the rainfall over these regions. Overall, the Merged product shows better performance in terms of POD and FAR compared to other products. Overall, all the satellite products show higher POD. The GSMaP-NRT and GSMaP-MVK shows higher POD and lower FAR compared to IMERG-NRT when averaged over Indian region. Prakash et al. (2016) also observed higher POD for GSMaP products than IMERG products, but the GSMaP have higher FAR than IMERG. Further, both the products of INSAT3D shows larger FAR over southeast peninsular India compared to other products. From the above analysis, it is clear that all the products except merged data have difficulty in rainfall detection. Figures 8 and 9 shows the spatial distributions of FBI and CSI, respectively, over the Indian sub-continent. All these data sets except IMERG show over detection of rainfall over the southeast peninsula, J&K and parts of north-western regions. The overshooting is more in INSAT3D compared to other data. It also shows a relatively larger region indicating over detection. The IMERG product also shows over detection similar to other products (Merged and GSMaP); however, the magnitude is less over J&K. IMERG-NRT shows better performance than other products over J&K and

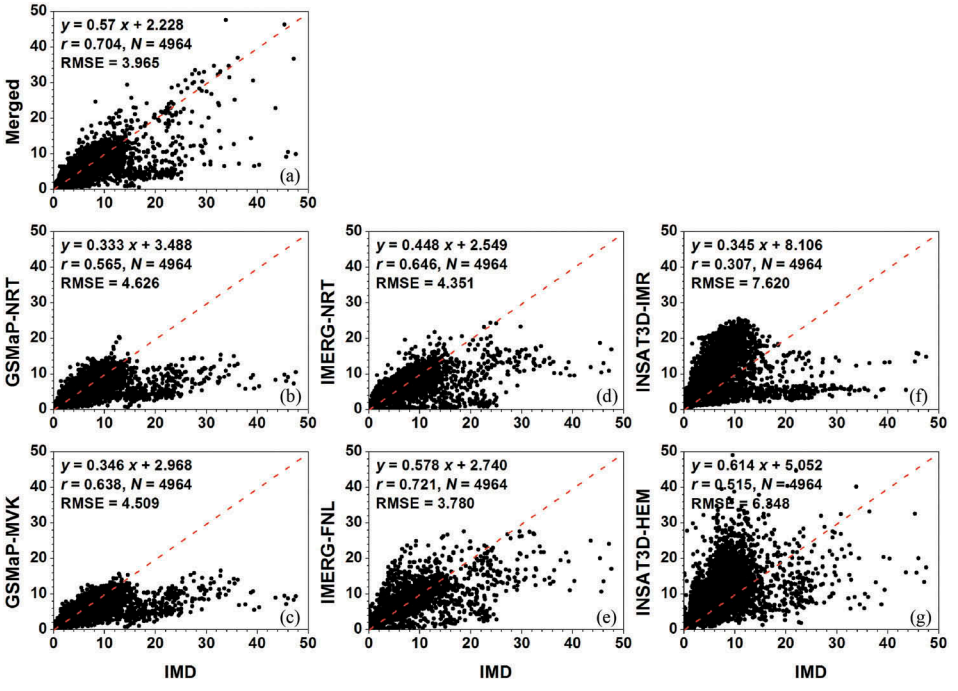

Figure 5. Scatter plots of averaged daily June–September rainfall (mm day^{-1}) over India from (a) Merged, (b) GSMaP-NRT, (c) GSMaP-MVK, (d) IMERG-NRT, (e) IMERG-FNL, (f) INSAT3D-IMR and (g) INSAT3D-HEM products of with respect to IMD data. Dashed lines represent 1:1 line and number of points (***N***), Correlation coefficient (*r*) and RMSE are also given in each plot.

Merged data shows better performance over WG in terms of FBI. CSI for all products shows higher magnitude over foothills of Himalayas, NE regions, central India and along WG regions and lower values in J&K and south peninsular India. Both the GSMaP products show lower CSI (<0.6) values over WG region compared to Merged and IMERG data products. These results show that the satellite-based rainfall products have difficulty in rainfall detection primarily over the J&K and southern peninsular India.

3.2. *Evaluation of high-resolution rainfall products at the all-India scale*

In this section, the gridded rainfall data sets are compared with the IMD observed rainfall data set over whole Indian region (spatial average) during the summer monsoon season 2016. The mean rainfall from June to September over whole of India is considered as all-India summer monsoon rainfall (AISMR). Figure 10 shows the time series of daily AISMR for IMD, GSMaP-NRT, GSMaP-MVK, IMERG-NRT, IMERG-FNL, INSAT3D-IMR, and INSAT3D-HEM data sets. It is clear from this figure that the Merged, GSMaP-NRT, GSMaP-MVK, IMERG-NRT and IMERG-FNL products produced almost similar rainfall compared to IMD observed rainfall. The lower rainfall amounts during June and September are well represented by these three satellite products. However, it underestimated the rainfall as compared to the gauge-based products during July and August. Both the INSAT3D products (IMR and HEM) overestimated the rainfall throughout the season. This can be

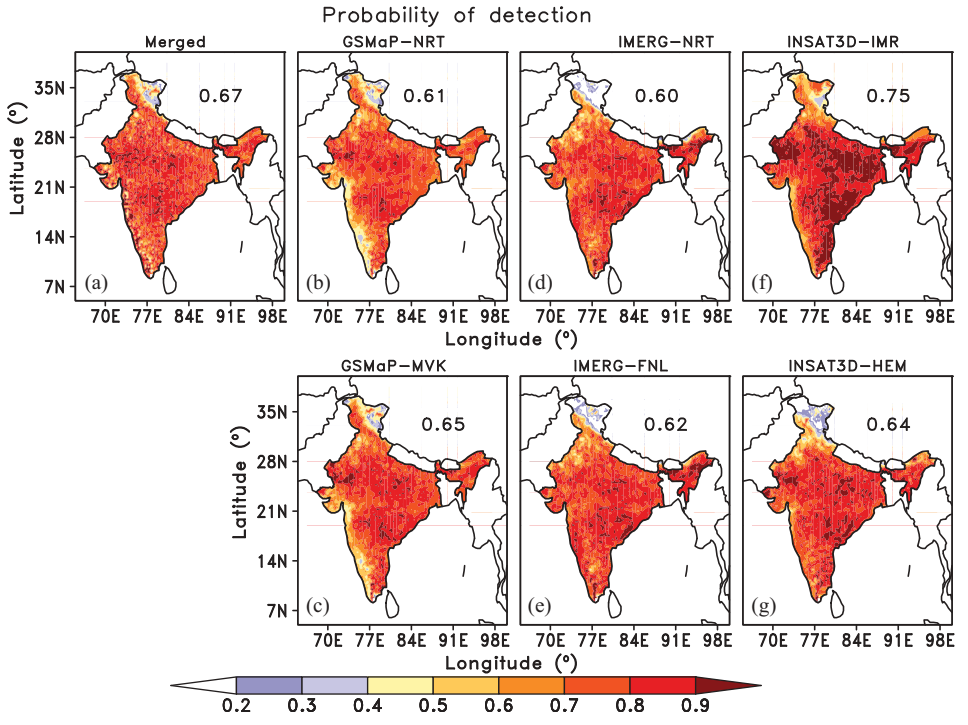

Figure 6. Spatial distributions of probability of detection (POD) during the southwest monsoon (JJAS 2016) over India from (a) Merged, (b) GSMaP-NRT, (c) GSMaP-MVK, (d) IMERG-NRT,(e) IMERG-FNL, (f) INSAT3D-IMR and (g) INSAT3D-HEM products with respect to IMD-SRG data. Mean values of POD averaged over India are also given in the parentheses.

further seen from the positive bias shown in Figure 11 by the INSAT3D products during the summer monsoon. GPM is designed for better tropical precipitation estimation (Huffman et al. (2015). The GPM core observatory carries 13-channel passive microwave radiometer, namely, GMI, and the first space-borne Dual frequency Precipitation Radar (DPR; the K_u-band at 13.6 GHz and K_a-band at 35.5 GHz). The main advantage of the DPR is its increased sensitivity to the lower rainfall (less than 0.5 mm hour^{-1}) and high-latitude snowfall measurements. In addition, the DPR can detect and estimate extreme precipitation more precisely. Hence, the intra-seasonal time scale variability of the monsoon rainfall is well captured by Merged, GSMaP-NRT, GSMaP-MVK, IMERG-NRT and IMERG-FNL products compared to INSAT3D-IMR and INSAT3D-HEM products.

Figure 11 shows the daily time series of bias in all India mean monsoon rainfall from Merged, GSMaP-NRT, GSMaP-MVK, IMERG-NRT, IMERG-FNL, INSAT3D-IMR, and INSAT3D-HEM products with the IMD gridded data set. The Merged data set shows positive bias during the first week of June. The bias in the estimation of rainfall by Merged product becomes negative from the second week of June onwards. This indicates that the Merged product underestimated the daily mean monsoon rainfall over India from 2nd week of June. The GSMaP products also show positive bias initially (upto the second week of June) and become negative thereafter. However, the magnitude of the bias is more in GSMaP products. The IMERG-NRT also shows similar bias as seen in GSMaP

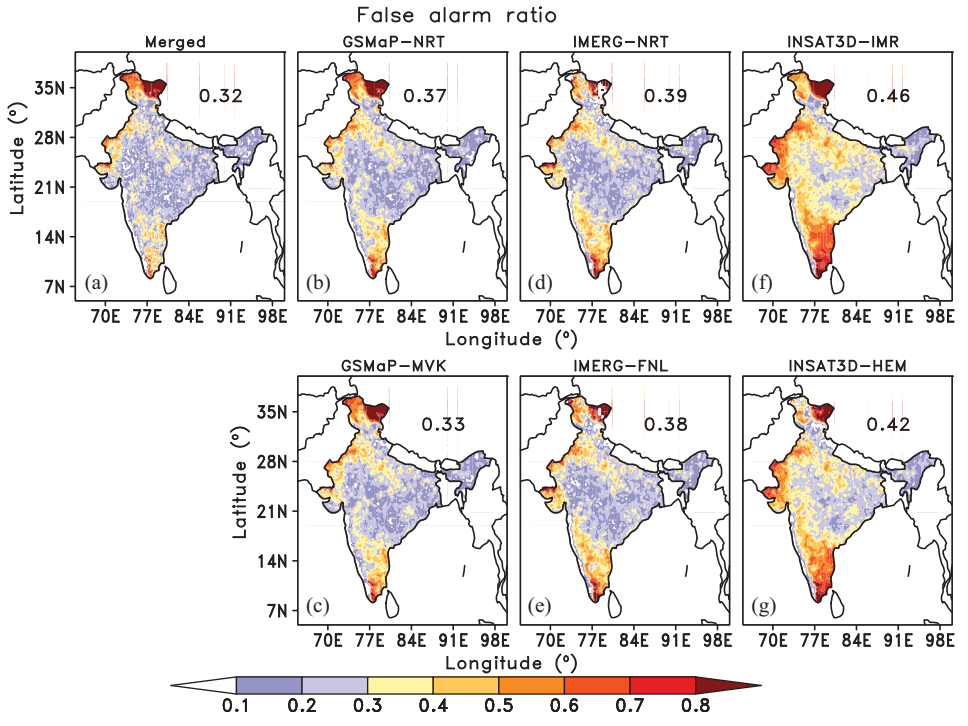

Figure 7. Spatial distributions of false alarm ratio (FAR) during the southwest monsoon (JJAS 2016) over India from (a) Merged, (b) GSMaP-NRT, (c) GSMaP-MVK, (d) IMERG-NRT,(e) IMERG-FNL, (f) INSAT3D-IMR and (g) INSAT3D-HEM products with respect to IMD-SRG data. Mean values of FAR averaged over India are also given in the parentheses.

products also. Whereas the IMERG-FNL shows systematic positive and negative biases with IMD gridded data set. The INSAT3D data products show positive values with higher magnitude of bias when compared against the IMD gridded data set. Prakash et al. (2014) also observed an underestimation of all India seasonal mean rainfall for most of the high-resolution satellite products. In all the seven data products, Merged and IMERG-FNL shows minimum bias with the IMD gridded dataset. Overall, in daily scale, the results reveal that Merged data product underestimated the rainfall after the second week of June and IMERG-FNL data shows systematic underestimation (3.23%) when averaged for the season. Whereas, the Merged data set shows 10% of underestimation when averaged for the whole season.

In Figure 12, variations in POD, FAR, FBI, and CSI of the satellite-based rainfall data sets for different daily rainfall threshold over India are shown with respect to IMD gauge-based data set. POD gradually decreases and FAR increases faster for all the rainfall data sets with the increased threshold values of daily rainfall. POD for GSMaP-NRT drops rapidly for higher thresholds. IMERG-NRT has lower POD values than IMERG-FNL, but higher than GSMaP datasets for higher rainfall threshold values. The INSAT3D-IMR shows higher POD for lower rainfall threshold (below 20 mm) and Merged product shows better POD for higher rainfall threshold (above 20 mm). In FAR, Merged product shows lower magnitude than others at all threshold values. INSAT3D-IMR shows higher FAR values for all rainfall

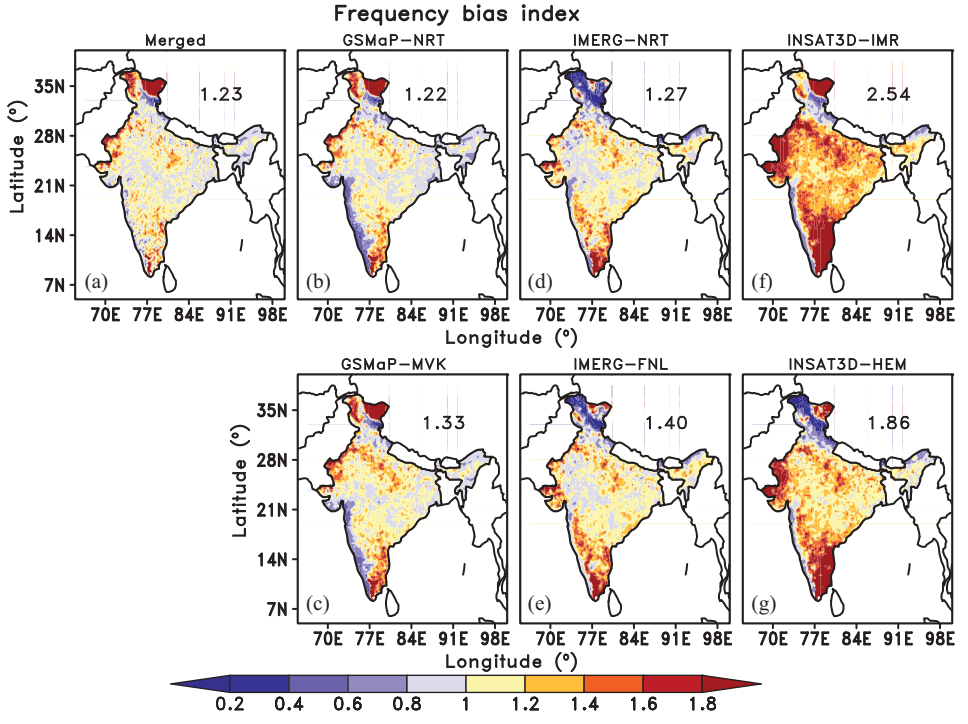

Figure 8. Spatial distributions of frequency bias index (FBI) during the southwest monsoon (JJAS 2016) over India from (a) Merged, (b) GSMaP-NRT, (c) GSMaP-MVK, (d) IMERG-NRT,(e) IMERG-FNL, (f) INSAT3D-IMR and (g) INSAT3D-HEM products with respect to IMD-SRG data. Mean values of FBI averaged over India are also given in the parentheses.

thresholds compared to all other data sets. FBI increases faster with increase of rainfall threshold (FBI even more than 2.0) for INSAT3D products. However, the remaining products show lower FBI values. Hence, INSAT3D products over detect the heavy rainfall events. The CSI values decrease with the increase in the rainfall threshold values for all the data products. The CSI value is higher (lower) for Merged (INSAT3D-IMR) data product for all the rainfall threshold values. Overall, Merged data set perform better than other data set for higher thresholds and categories of daily rainfall.

3.3. *Evaluation of high-resolution rainfall products at regional scale*

To observe the rainfall variability in different data products at regional scale, four regions are selected depending on variation of rainfall and orography (Figure 1(a)). Region 1 comprises the central India (CI) which covers the monsoon trough zone and has high rainfall variability during the summer monsoon. Region 2 contains the Western Ghats (WG), having highly complex orography with large east-west gradients of the monsoon rainfall on both sides of the WG Mountains. The windward side receives very heavy rainfall, whereas the leeward side gets low rainfall during the monsoon season. Region 3 shows the NE region of India with a hilly terrain different from WG and receives very heavy rainfall during the monsoon season. Region 4 includes the interior peninsular

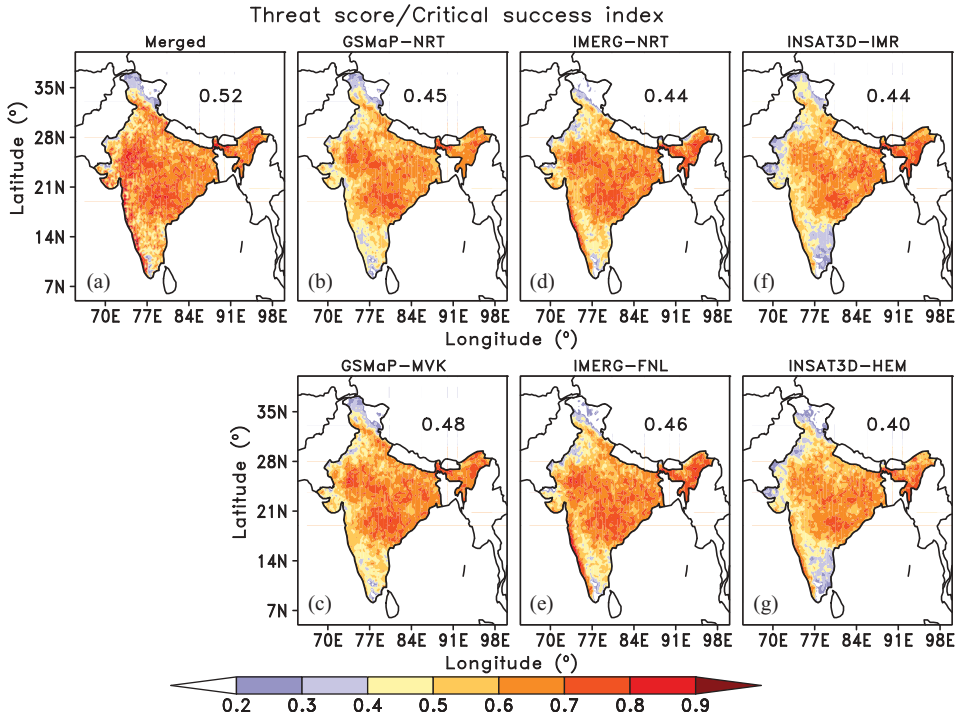

Figure 9. Spatial distributions of threat score (TS) during the southwest monsoon (JJAS 2016) over India from (a) Merged, (b) GSMaP-NRT, (c) GSMaP-MVK, (d) IMERG-NRT,(e) IMERG-FNL, (f) INSAT3D-IMR and (g) INSAT3D-HEM products with respect to IMD-SRG data. Mean values of TS averaged over India are also given in the parentheses.

India (PI). The monthly means of daily accumulated gridded rainfall data along with correlation coefficient, bias and RMSE for region 1 (CI) during the summer monsoon months (June to September) are shown in Figure 13. The daily accumulated rainfall is minimum (4.59 mm day^{-1}) during the month of June and increases to a maximum (11.57 mm day^{-1}) during July and declines during August and September. Merged and IMERG data products captures well these monthly variations compared to other data sets. The INSAT3D datasets show higher mean rainfall over these monsoon months in central India. The bias is positive indicating overestimation of rainfall for all the datasets during June. Merged, GSMaP-NRT, and IMERG-NRT show negative bias during July to September over central India. Among all the datasets, IMERG-FNL shows minimum bias (<0.6 mm day^{-1}) over central India. However, the INSAT3D data products show high (>3 mm day^{-1}) and positive bias during monsoon month in central India. Similarly, the RMSE ('*r*') is minimum (higher) for Merged, GSMaP-NRT, IMERG-NRT, and IMERG-FNL over all the monsoon months. However, the merged product shows less bias (−0.9%) and RMSE (18%) along with high '*r*' (0.93) compared to other satellite products over central India (Table 2). Figure 14 presents the monthly means of daily accumulated rainfall along with correlation coefficient, bias and RMSE for region 2 (WG) during monsoon months. WG region receives maximum (13.36 mm day^{-1}) rainfall during peak monsoon months (July) and minimum (5.74 mm day^{-1}) during the month of September due to the

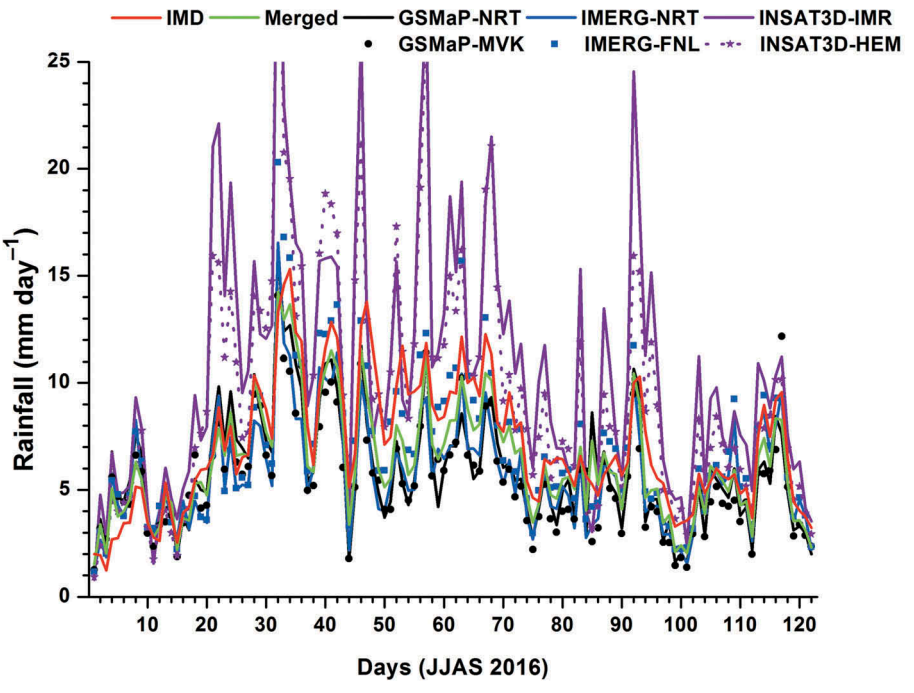

Figure 10. Time series of daily all-India summer monsoon rainfall (mm day^{-1}) for 2016 from IMD rain gauge, Merged, GSMaP-NRT, GSMaP-MVK, IMERG-NRT, IMERG-FNL, INSAT3D-IMR and INSAT3D-HEM products.

withdrawal phase of the monsoon. All the seven data products show underestimation of rainfall over WG region. The merged product shows less bias (−16%), low RMSE (24%) and high '*r*' (0.97) among other satellite products. However, the INSAT3D-IMR shows less '*r*' (<0.6 mm day^{-1}) compared to other data products in region2 (Table 2).

Similarly, the monthly means of daily accumulated rainfall along with correlation coefficient, bias and RMSE for region 3 (NE region of India) and region 4 (peninsular India) are reported in Figures 15 and 16. NE region receives on an average higher rainfall over monsoon months compared to other regions. In monsoon 2016, the maximum (20.56 mm day^{-1}) daily accumulated rainfall was recorded during July and minimum (6.93 mm day^{-1}) during August. All the seven data products show higher and negative biases during the months of June, July and September over this region indicating the underestimation of rainfall in this region. All the data products except INSAT3D data product show very small biases during the month of August. The RMSE also minimum in August compared to other months. The '*r*' is higher for all the data products except for INSAT3D data product in this region. Merged data product shows better results with less bias, RMSE and high '*r*' over NE region compared to other data products. In the NE region, the IMERG-FNL shows less bias (−23.4%) and RMSE (54%) and high '*r*' (0.7) compared to other products (Table 2).

The peninsular India (PI) receives rather less rainfall compared to other regions during the monsoon months. The mean daily accumulated rainfall is comparable for all the monsoon months in this region. The IMERG data products capture better the observed

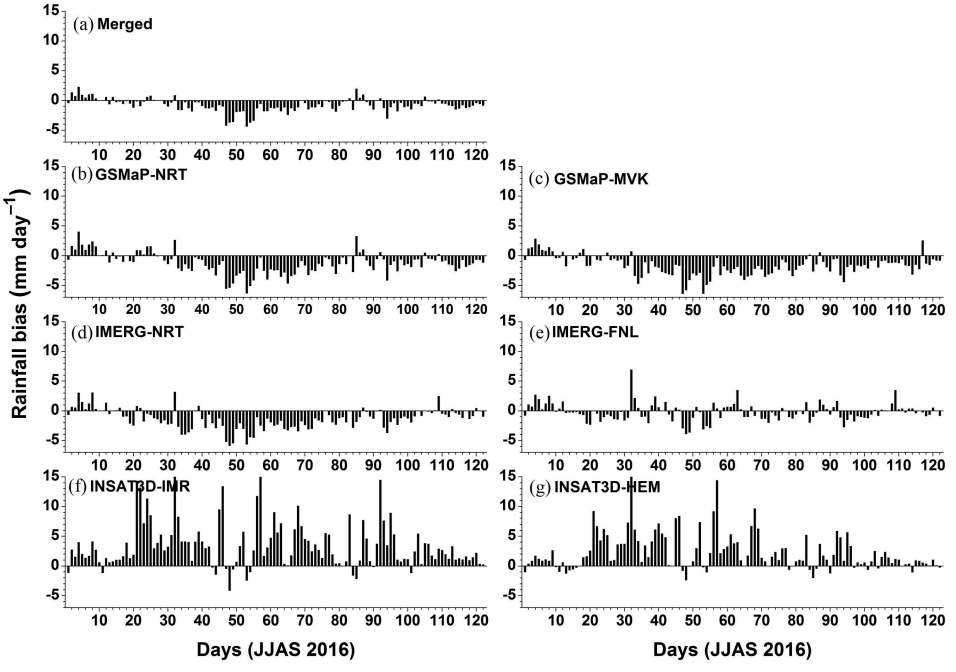

Figure 11. Time series of daily all-India summer monsoon rainfall bias (mm day^{-1}) for 2016 from (a) Merged, (b) GSMaP-NRT, (c) GSMaP-MVK, (d) IMERG-NRT, (e) IMERG-FNL, (f) INSAT3D-IMR and (g) INSAT3D-HEM products with respect to IMD-SRG data.

rainfall during the month of June. Whereas other data products show higher rainfall during this month. In remaining months, all the data products agree with the observed rainfall except INSAT3D. For all products except INSAT3D, the bias in the estimation of mean daily rainfall is minimum (close to zero) during the months of July, August and September. Further, the bias is higher for June for all the data products except IMERG-NRT data product. Similar to the bias, the RMSE is also less in July compared to other monsoon months. Among all the data products, the Merged data product shows minimum RMSE and INSAT3D data product shows higher RMSE values in all the months. The '*r*' of all the data products are comparable to one another in this region with higher values of '*r*' is observed for Merged data product and lower values for INSAT3D data products. In this region, IMERG-FNL captures better with smaller bias (0.08%), and Merged product shows lower RMSE (44%) and high '*r*' (0.94) (Table 2).

Several studies have been conducted to elucidate the accuracy of precipitation products over various geographical regions of India. Prakash et al. (2016a) evaluated the TMPA and GSMaP Products over India using IMD observations and found that these products show poor performance over the WG and over southeast peninsular India. The IMERG, TMPA, and GSMaP multi-satellite rainfall estimates show comparable correlation over India and three sub-regions, except over the NE region of India, where both IMERG and GSMaP show relatively smaller correlation and larger RMSE as compared with TMPA rainfall estimates (Prakash et al. 2016). There it is also shown that, IMERG and GSMaP have a larger negative total bias over the NE region of India. In the present study, IMERG-NRT, and GSMaP-NRT rainfall estimates show comparable correlation over Indian

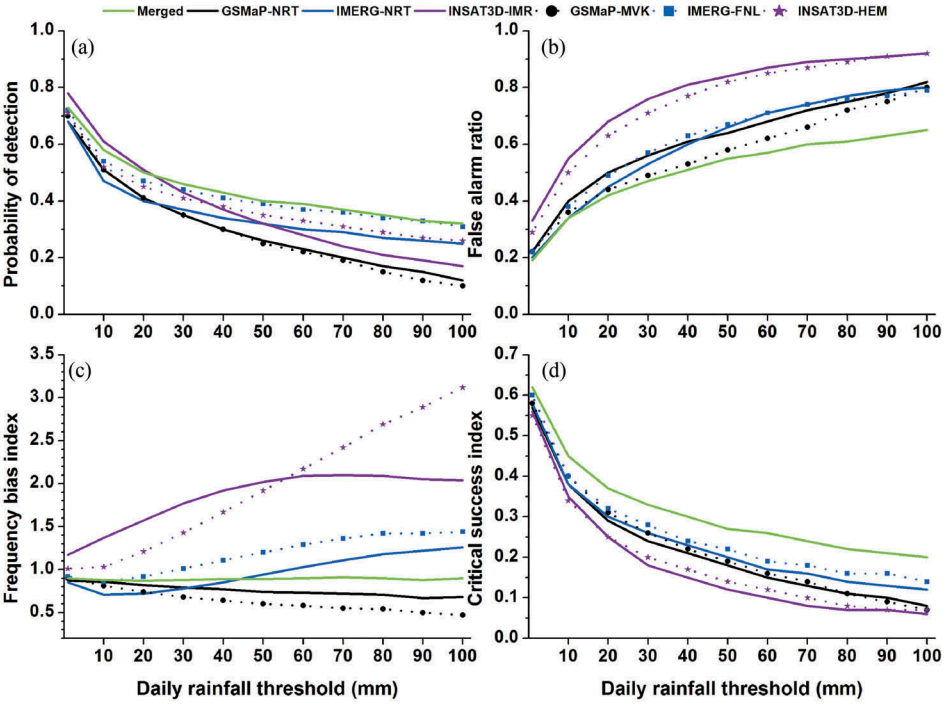

Figure 12. Variations of POD, FAR, FBI, and CSI as a function of different daily JJAS 2016 rainfall threshold over India from merged, GSMaP-NRT, GSMaP-MVK, IMERG-NRT, IMERG-FNL, INSAT3D-IMR and INSAT3D-HEM products with respect to IMD-SRG data.

region, except over the NE region of India where both IMERG-NRT and GSMaP-NRT show relatively smaller correlation and larger RMSE. Among these two measurements, IMERG-NRT shows less bias and RMSE with higher correlation compared to GSMaP-NRT over the NE region of India. The total bias/error and its components show that TMPA and IMERG have a total bias of the order of 20% over the southeast peninsular India, which is much higher than that for GSMaP (Prakash et al. 2016) where they used version3 for IMERG. The total bias in IMERG-NRT and GSMaP-NRT are 5% and 26% over south peninsular India. This is also an evident that the IMERG V04 shows much improvement compared to IMERG V03.

Nair, Srinivasan, and Nemani (2009) examined the performance of TMPA product over the western states of India and found that the TMPA product fails to detect the heavy convective precipitation, particularly over the windward side of the Western Ghats. TRMM-3B42V7, CPC-RFE2.0 gauge-adjusted multi-satellite rainfall products show larger RMSE of the order of 100% along the west coast of India (Prakash et al. 2015). This shows that the accurate estimation by satellite-based precipitation products remains a challenging task especially over mountainous regions. Our results indicate that, the gauge-adjusted multi-satellite rainfall products, IMERG-FNL and Merged products shows 10% overestimation and 15% underestimation, respectively, in rainfall estimation with RMSE of the order of 50% and 25% over WG. This indicates that the recent versions of IMERG estimates are improved even in orographic regions. This study provides regional

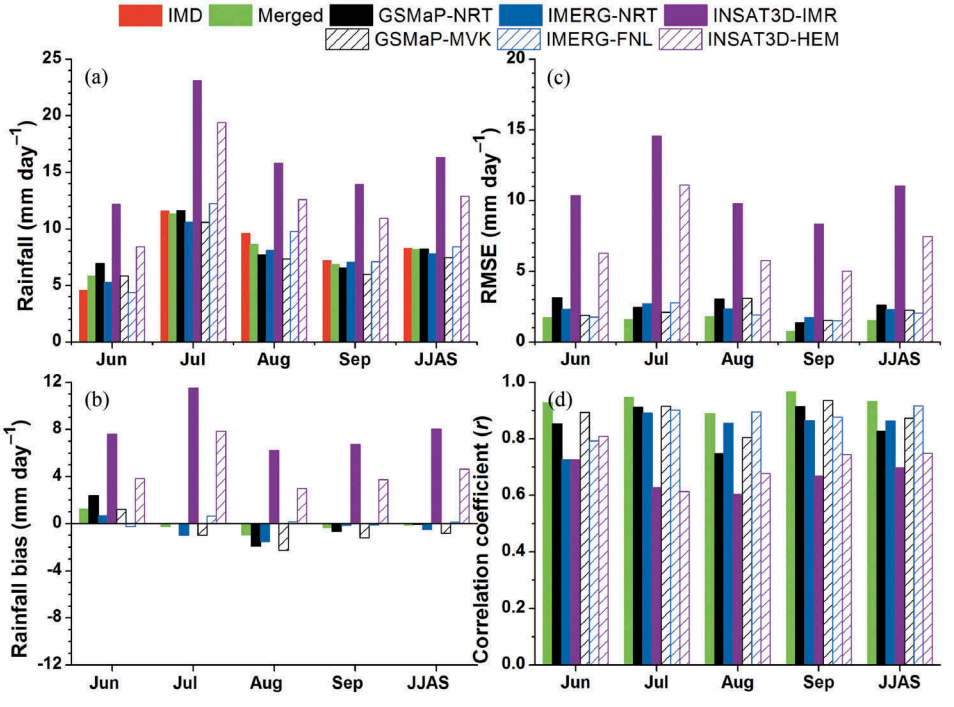

Figure 13. Time series of monthly and season wise over central India (CI) summer monsoon (a) mean rainfall (mm day^{-1}), (b) bias (mm day^{-1}), (c) RMSE (mm day^{-1}) and (d) Correlation coefficient (*r*) for 2016 from IMD rain gauge, Merged, GSMaP-NRT, GSMaP-MVK, IMERG-NRT, IMERG-FNL, INSAT3D-IMR and INSAT3D-HEM products.

Table 2. Statistical indices of percentage bias (P Bias), percentage RMSE (P RMSE) and correlation coefficient (*r*) during the southwest monsoon (JJAS 2016).

	Merged	GSMa-PNRT	IMERG-NRT	INSAT3D-IMR	GSMa-PMVK	IMERG-FNL	INSAT3D-HEM
All India							
P Bias (%)	−11.23	−17.27	−18.96	49.30	23.31	−3.23	33.29
P RMSE (%)	19.66	30.75	30.67	75.32	33.18	21.61	58.03
r	0.92	0.80	0.82	0.77	0.83	0.89	0.84
Central India							
P Bias (%)	−0.978	−0.628	−5.918	97.004	−9.795	1.618	55.791
P RMSE (%)	18.565	31.392	27.841	133.313	27.140	24.845	90.095
r	0.932	0.826	0.863	0.697	0.873	0.917	0.749
Western Gats of India							
P Bias (%)	−16.235	−50.121	−37.401	−43.154	−48.991	9.922	15.106
P RMSE (%)	24.311	69.587	58.967	78.264	68.711	53.974	74.664
r	0.975	0.752	0.782	0.510	0.753	0.864	0.777
North-East of India							
P Bias (%)	−46.465	−55.351	−44.751	−35.176	−56.201	−23.456	−13.530
P RMSE (%)	71.093	84.763	72.031	80.133	85.729	54.706	65.592
r	0.746	0.426	0.645	0.269	0.408	0.730	0.509
Peninsula of India							
P Bias (%)	15.640	26.523	5.560	141.89	18.852	0.089	54.891
P RMSE (%)	44.424	86.083	62.652	208.712	63.574	48.914	106.095
r	0.945	0.829	0.918	0.791	0.914	0.931	0.829

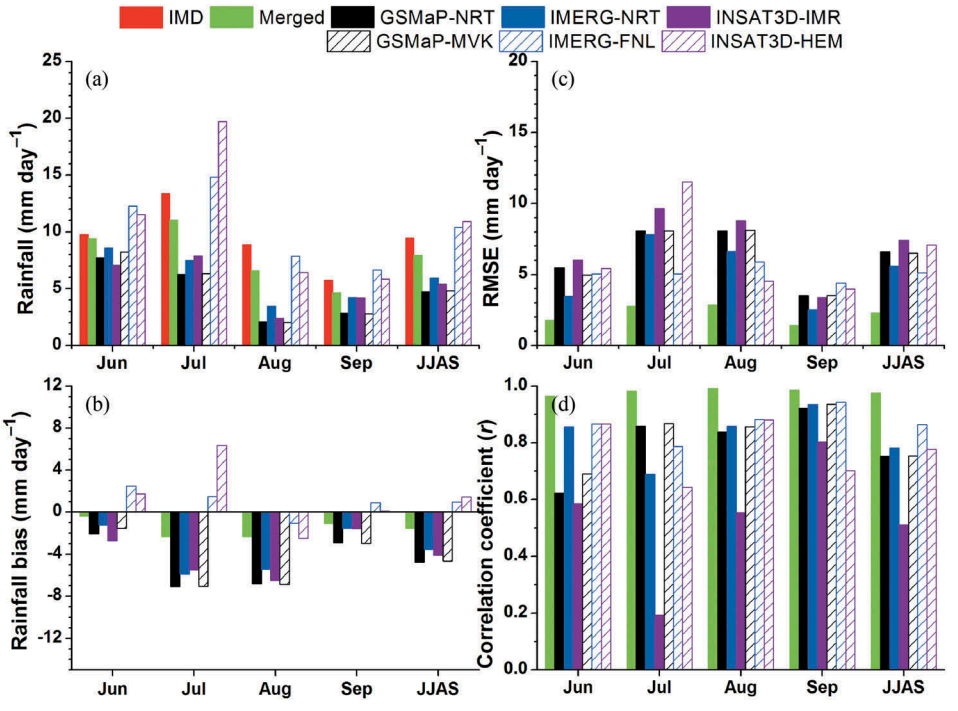

Figure 14. Time series of monthly and season wise over Western Gats (WG) summer monsoon (a) mean rainfall (mm day^{-1}), (b) bias (mm day^{-1}), (c) RMSE (mm day^{-1}) and (d) Correlation coefficient (*r*) for 2016 from IMD rain gauge, Merged, GSMaP-NRT, GSMaP-MVK, IMERG-NRT, IMERG-FNL, INSAT3D-IMR and INSAT3D-HEM products.

assessment for GPM precipitation to users and also provides feedback to IMERG algorithm developers.

Above performance analysis indicates that the distribution of precipitation in IMERG and GSMaP has improved markedly, especially for light rainfall. However, all the satellite-based rainfall estimates indicate exceptionally smaller correlation coefficient, larger RMSE, higher total bias over the NE region of India where higher precipitation is caused due to orographic effects. INSAT3D measurements show higher positive bias and RMSE over peninsular of India, and less bias and RMSE over north-east India. The more important aspect of INSAT3D measurements is its high temporal (at every 30-min interval) availability of data sets. Hence, further improvements are needed for better estimation of rainfall in particularly for operational scientific works for applications in natural disasters, and now casting. The climatic conditions of the Indian region have much more diversity with different types of clouds and a wide range of precipitation rates during monsoon season. In this scenario, we expect this investigation provides the satellite precipitation users a better understanding of the features associated with currently available multi-satellite precipitation estimates.

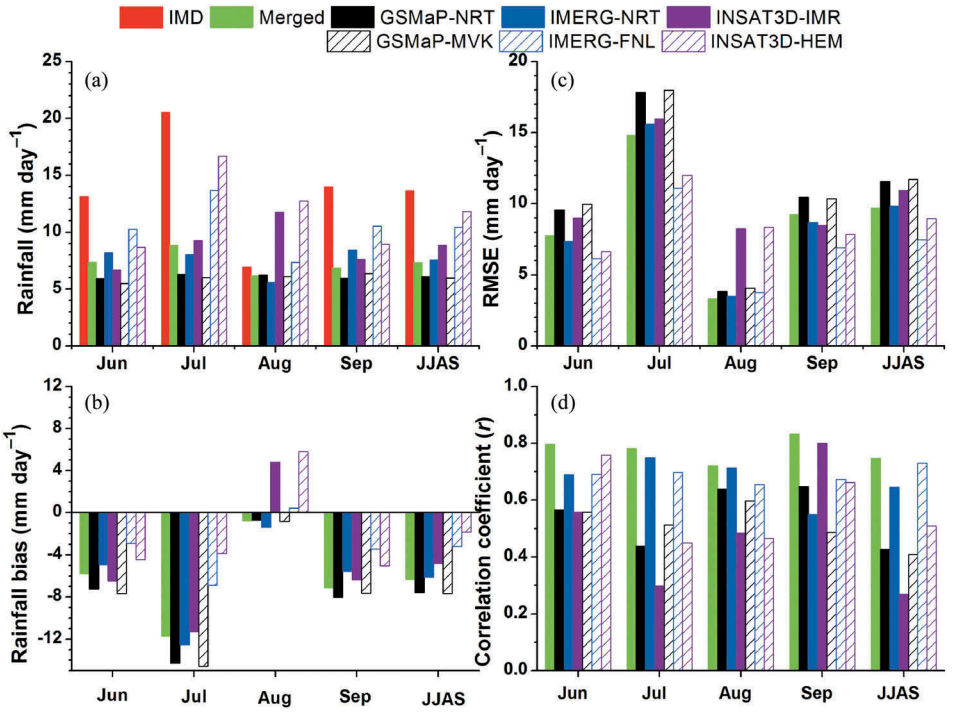

Figure 15. Time series of monthly and season wise over North-East (NE) India summer monsoon (a) mean rainfall (mm day^{-1}), (b) bias (mm day^{-1}), (c) RMSE (mm day^{-1}) and (d) Correlation coefficient (*r*) for 2016 from IMD rain gauge, Merged, GSMaP-NRT, GSMaP-MVK, IMERG-NRT, IMERG-FNL, INSAT3D-IMR and INSAT3D-HEM products.

4. Summary and conclusion

Rainfall from GPM mission and Indian National Satellite measurements are comprehensively evaluated against IMD gauge-based measurements over Indian region. The daily rainfall measured by Merged, GSMaP, IMERG, and INSAT3D have been evaluated during the summer monsoon period from June to September, 2016. The spatial distributions of mean monsoon rainfall showed that the merged and IMERG data products captured the large-scale Indian monsoon rainfall features realistically. The NRT and MVK products of GSMaP show similar rainfall patterns over the Indian region. Further, there exist significant differences between GSMaP-NRT and IMERG-NRT, whereas, the INSAT3D data products overestimated the mean rainfall and GSMaP underestimated over most of the regions on monthly as well as seasonal scales. Especially, INSAT3D-IMR and INSAT3D-HEM depicts over-estimation of rainfall relatively over larger region. Among these two products, HEM shows 15% better performance than IMR. The time series of daily all Indian summer monsoon rainfall shows that the Merged and IMERG-FNL products produce similar rainfall compared with the IMD gauge rainfall. IMERG-FNL and Merged datasets show 3% and 11% underestimation when averaged for the whole season.

In addition, various continuous skill metrics such as correlation coefficient, RMSE, and traditional skill scores such as POD, FAR, FBI, and CSI were calculated to assess the

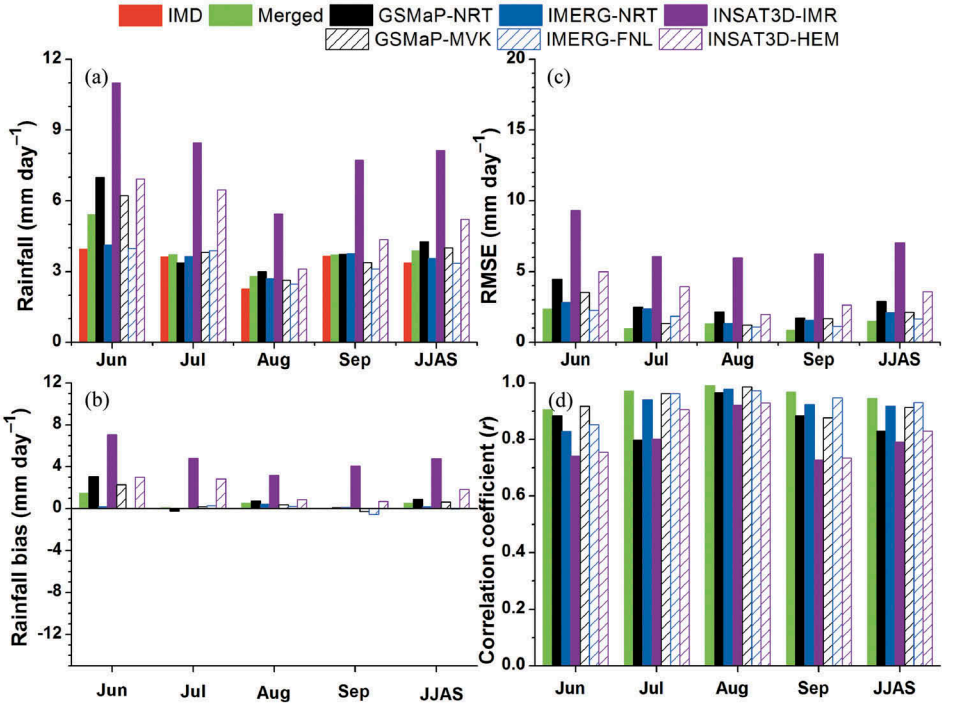

Figure 16. Time series of monthly and season wise over interior peninsula India (PI) summer monsoon (a) mean rainfall (mm day^{-1}), (b) bias (mm day^{-1}), (c) RMSE (mm day^{-1}) and (d) Correlation coefficient (*r*) for 2016 from IMD rain gauge, Merged, GSMaP-NRT, GSMaP-MVK, IMERG-NRT, IMERG-FNL, INSAT3D-IMR and INSAT3D-HEM products.

capability of satellite-based rainfall products in rainfall estimation over India. Merged data products show better skills in representing the rainfall, whereas INSAT3D products depict lower skill metrics. GPM-based products such as IMERG and GSMaP are better than INSAT3D estimation. All the satellite-based measurements show better POD (>0.7) over most of the India regions. However, these satellite-based measurements have uncertainty in the detection of precipitation primarily over complex topography (WG and foothills of Himalayas) and J&K regions.

The comparison of the sub-regional scale showed that even though all the datasets were able to capture the seasonal variability reasonably well, there were considerable regional differences among them in terms of bias and RMSE. Merged product shows lower bias (−0.9%) and RMSE (18%) and higher '*r*' (0.93) compared to other products over Central India. The HEM product of INSAT3D shows 13% underestimation (lower bias compared to other satellite measurements) over NE region of India, whereas it overestimated in other regions. GSMaP underestimated the rainfall over all the regions except South Peninsular India where it shows higher '*r*'. The Merged data product shows 15% underestimation and IMERG-FNL data products show 10% overestimation of rainfall over WG. The better performance of IMERG-FNL data set can be attributed due to the gauge adjusted measurements in IMERG-FNL. The present study shows that the IMERG V04 products improved compared to IMERG V03, especially over orographic regions. Overall, the Merged and

IMERG-FNL products show better performance compared to other satellite products, as these data sets are generated by using the gauge data.

The present study shows that the accurate estimation of satellite precipitation remains a challenging task. This may be due to the insufficient number of gauges which are used for bias correction in satellite products. The assessment of the present report can throw light on different satellite-based precipitation estimate which are currently available for Indian region. These results provide feedback to the algorithm developers for further improvements in multi-satellite precipitation estimation.

Acknowledgments

The authors would like to acknowledge the INSAT Meteorological Data Processing System (IMDPS) of Space Application Centre (SAC) for supplying the INSAT3D data. The authors also acknowledge the JAXA, JAPAN and NASA, USA for the provision of GPM dataset. NCMRWF part of the work is under MoES-NERC INCOMPASS project. Thanks are due to the Head, NCMRWF for his engorgement in this study.

Disclosure statement

No potential conflict of interest was reported by the authors.

References

Adler, R. F., and A. J. Negri. 1988. "A Satellite Infrared Technique to Estimate Tropical Convective and Stratiform Rainfall." *Journal of Applied Meteorology* 27 (1): 30–51. doi:10.1175/1520-0450-(1988)027<0030:ASITTE>2.0.CO;2.

Aonashi, K., J. Awaka, M. Hirose, T. Kozu, T. Kubota, G. Liu, S. Shige, et al. 2009. "GSMaP Passive Microwave Precipitation Retrieval Algorithm: Algorithmdescription and Validation". *Journal of the Meteorological Society of Japan. Ser. II* 87: 119–136. doi:10.2151/jmsj.87A.119.

Arkin, P. A., and P. Xie. 1994. "The Global Precipitation Climatology Project: First Algorithm Intercomparison Project." *Bulletin of the American Meteorological Society* 75 (3): 401–419. doi:10.1175/1520-0477(1994)0752.0.CO;2.

Arkin, P. A., R. Joyce, and J. E. Janowiak. 1994. "The Estimation of Global Monthly Mean Rainfall Using Infrared Satellite Data: The GOES Precipitation Index (GPI)." *Remote Sensing Reviews* 11 (1–4): 107–124. doi:10.1080/02757259409532261.

Asong, Z. E., S. Razavi, H.S. Wheater, and J.S. Wong. 2017. "Evaluation Of Integrated Multisatellite Retrievals for Gpm (Imerg) over Southern Canada against Ground Precipitation Observations: a Preliminary Assessment." *Journal Of Hydrometeorology* 18: 1033-1050.

Ba, M. B., and A. Gruber. 2001. "GOES Multispectral Rainfall Algorithm (GMSRA)." *Journal of Applied Meteorlogy* 40: 1500–1514. doi:10.1175/1520-0450(2001)040<1500:GMRAG>2.0.CO;2.

Chen, F., and Li. Xi. 2016. "Evaluation Of Imerg and Trmm 3b43 Monthly Precipitation Products over Mainland China." *Remote Sensing* 8 (6): 472.

Cressman, G. P. 1959. "An Operational Objective Analysis System." *Monthly Weather Review* 87: 367–374. doi:10.1175/1520-0493(1959)087<0367:AOOAS>2.0.CO;2.

Dinku, T., F. Ruiz, S. J. Connor, and P. Ceccato. 2009. "Validation and Intercomparison of Satellite Rainfall Estimates over Colombia." *Journal of Applied Meteorology and Climatology* 49: 1004–1014. doi:10.1175/2009JAMC2260.1.

Ferraro, R. R., F. Weng, N. C. Grody, L. Zhao, H. Meng, C. Kongoli, P. Pellegrino, S. Qiu, and C. Dean. 2005. "NOAA Operational Hydrological Products Derived from the Advanced Microwave

Sounding Unit." *IEEE Transactions on Geoscience and Remote Sensing* 43 (5): 1036–1048. doi:10.1109/TGRS.2004.843249.

Gaona, M. R., A. Overeem, H. Leijnse, and R. Uijlenhoet. 2016. "First-year Evaluation Of Gpm Rainfall over The Netherlands: Imerg Day 1 Final Run (V03d)." *Journal Of Hydrometeorology* 17 (11): 2799–2814.

Guo, H., S. Chen, A. M. Bao, A. Behrangi, Y. Hong, F. Ndayisaba, J. J. Hu, and P. M. Stepanian. 2016. "Early Assessment Of Integrated Multi-satellite Retrievals for Global Precipitation Measurement over China." *Atmospheric Research* 176: 121–133.

Hogan, R. J., C. A. T. Ferro, I. T. Jolliffe, and D. B. Stephenson. 2010. "Equitability Revisited." *Why The "Equitable Threat Score" Is Not Equitable." Weather and Forecasting* 25: 710–726. doi: 10.1175/2009WAF2222350.1.

Hong, Y., K.-L. Hsu, S. Sorooshian, and X. Gao. 2004. "Precipitation Estimation from Remotely Sensed Imagery Using an Artificial Neural Network Cloud Classification System." *Journal of Applied Meteorlogy* 43: 1834–1853. doi:10.1175/JAM2173.1.

Hou, A. Y., G. Skofronick-Jackson, C. D. Kummerow, and J. M. Shepherd. 2008. "Global Precipitation Measurement." In *Precipitation: Advances in Measurement, Estimation and Prediction*, edited by S. Michaelides, 131–169. Berlin: Springer.

Hou, A. Y., R. K. Kakar, S. Neeck, A. A. Azarbarzin, C. D. Kummerow, M. Kojima, R. Oki, K. Nakamura, and T. Iguchi. 2014. "The Global Precipitation Measurement Mission." *Bulletin of the American Meteorological Society* 95: 701–722. doi:10.1175/BAMS-D-13-00164-1.

Huffman, G., D. Bolvin, D. Braithwaite, K. Hsu, R. Joyce, and P. Xie. 2015. "Integrated Multi-satellitE Retrievals for GPM (IMERG), Version 4.5."*NASA's Precipitation Processing Center*, Accessed 6 January 2016. http://pmm.nasa.gov/sites/default/files/document_files/IMERG_ATBD_V4.5.pdf International Geophysics Series.

Huffman, G. J., D. T. Bolvin, E. J. Nelkin, D. B. Wolff, R. F. Adler, G. Gu, Y. Hong, K. P. Bowman, and E. F. Stocker. 2007. "The TRMM Multisatellite Precipitation Analysis (TMPA): Quasi-Global, Multiyear, Combined-Sensor Precipitation Estimates at Fine Scales." *Journal of Hydrometeorology* 8: 38–55. doi:10.1175/JHM560.1.

Huffman, G. J., R. F. Adler, D. T. Bolvin, and E. J. Nelkin. 2010. "The TRMM multi-satellite precipitation analysis (TMPA)." In Satellite Applications for Surface Hydrology, edited by F. Hossain and M. Gebremichael, 3–22. New York, NY: Springer. ISBN:978–90–481–2914–0.

Huffman, G.J., D.T. Bolvin, E.J. Nelkin, and E.F. Stocker, 2017. V04 IMERG Final Run Release Notes. NASA's Precipitation Processing Center, Accessed 21 March 2017. https://docserver.gesdisc.eosdis.nasa.gov/public/project/GPM/IMERG_FinalRun_V04_release_notes.pdf

Joyce, R. J., J. E. Janowiak, P. A. Arkin, and P. Xie. 2004. "CMORPH: A Method that Produces Global Precipitation Estimates from Passive Microwave and Infrared Data at High Spatial and Temporal Resolution." *Journal of Hydrometeorology* 5: 487–503. doi:10.1175/15257541(2004)005<0487:CAMTPG>2.0.CO;2.

Joyce, R. J., and P. Xie. 2011. "Kalman Filter-Based CMORPH." *Journal of Hydrometeorology* 12 (6): 1547–1563. doi:10.1175/JHM-D-11-022.1.

Kubota, T., S. Shige, H. Hashizume, K. Aonashi, N. Takahashi, S. Seto, Y. N Takayabu, et al. 2007. "Global Precipitation Map Using Satellite-Borne Microwave Radiometers by the GSMaP Project: Production and Validation." *IEEE Transactions on Geoscience and Remote Sensing* 45 (7): 2259–2275. doi:10.1109/TGRS.2007.895337.

Kubota, T., T. Ushio, S. Shige, S. Kida, M. Kachi, and K. Okamoto. 2009. "Verification of High Resolution Satellite-Based Rainfall Estimates around Japan Using a Gauge Calibrated Ground Radar Data Set." *Journal of Meteorological Society of Japan* 87A: 203–222. doi:10.2151/jmsj.87A.203.

Liu, Z. 2016. "Comparison of Integrated Multisatellite Retrievals for GPM (IMERG) and TRMM Multisatellite Precipitation Analysis (TMPA) Monthly Precipitation Products: Initial Results." *Journal of Hydrometeorology* 17: 777–790. doi:10.1175/JHM-D-15-0068.1.

Ma, Z. Y., G. Tang, D. Long, B. Yong, L. Zhong, W. Wan, and Y. Hong. 2016. "Similarity and Error Intercomparison of the GPM and Its Predecessor-TRMM Multisatellite Precipitation Analysis

Using the Best Available Hourly Gauge Network over the Tibetan Plateau." *Remote Sensing* 8: 569. doi:10.3390/rs8070569.

Mitra, A. K., A. K. Bohra, M. N. Rajeevan, and T. N. Krishnamurti. 2009. "Daily Indian Precipitation Analyses Formed from a Merge of Rain-Gauge with TRMM TMPA Satellite Derived Rainfall Estimates." *Journal of Meteorological Society of Japan* 87A: 265–279. doi:10.2151/jmsj.87A.265.

Mitra, A. K., I. M. Momin, E. N. Rajagopal, S. Basu, M. N. Rajeevan, and T. N. Krishnamurti. 2013. "Gridded Daily Indian Monsoon Rainfall for 14 Seasons: Merged TRMM and IMD Gauge Analyzed Values." *Journal of Earth System Science* 122: 1173–1182. doi:10.1007/s12040-013-0338-3.

Mitra, A. K., M. Dasgupta, S. V. Singh, and T. N. Krishnamurti. 2003. "Daily Rainfall for Indian Monsoon Region from Merged Satellite and Raingauge Values: Large-Scale Analysis from Realtime Data." *Journal of Hydrometerology* 4 (5): 769–781.

Mitra, A. K., N. Kaushik, S. Anil Kumar, S. Parihar, and S. C. Bhan. 2018. "Evaluation of INSAT-3D Satellite Derived Precipitation Estimates for Heavy Rainfall Events and Its Validation with Gridded GPM (IMERG) Rainfall Dataset over the Indian Region." *Remote Sensing Applications: Society and Environment* 9: 91–99. doi:10.1016/j.rsase.2017.12.006.

Murali Krishna, U. V., S. K. Das, S. M. Deshpande, S. L. Doiphode, and G. Pandithurai. 2017. "The Assessment of Global Precipitation Measurement Estimates over the Indian Subcontinent." *Earth and Space Science* 4: 540–553. doi:10.1002/2017EA000285.

Nair, S., G. Srinivasan, and R. Nemani. 2009. "Evaluation of Multi-Satellite TRMM Derived Rainfall Estimates over a Western State of India." *Journal of Meteorological Society of Japan. Ser. II* 87: 927–939. doi:10.2151/jmsj.87.927.

Pai, D. S., L. Sridhar, M. Rajeevan, O. P. Sreejith, N. S. Satbhai, and B. Mukhopadhyay. 2014. "Development of a New High Spatial Resolution (0.25° × 0.25°) Long Period (1901–2010) Daily Gridded Rainfall Data Set over India and Its Comparison with Existing Data Sets over the Region." *Mausam* 65 (1): 1–18.

Pai, D. S., L. Sridhar, M. R. Badwaik, and M. Rajeevan. 2015. "Analysis of the Daily Rainfall Events over India Using a New Long Period (1901–2010) High Spatial Resolution (0.25° × 0.25°) Gridded Rainfall Data Set." *Climate Dynamics* 45 (3–4): 755–776. doi:10.1007/s00382-014-2307-1.

Prakash, S., A. K. Mitra, A. AghaKouchak, Z. Liu, H. Norouzi, and D. S. Pai. 2016. "A Preliminary Assessment of GPM-based Multisatellite Precipitation Estimates over A Monsoon Dominated Region." *Journal of Hydrology*. doi:10.1016/j.jhydrol.2016.01.029.

Prakash, S., A. K. Mitra, and D. S. Pai. 2015. "Comparing Two High-Resolution Gauge-Adjusted Multisatellite Rainfall Products over India for the Southwest Monsoon Period." *Meteorological Applications* 22: 679–688. doi:10.1002/met.1502.

Prakash, S., A. K. Mitra, E. N. Rajagopal, and D. S. Pai. 2015. "Assessment of TRMM-based TMPA-3B42 and GSMaP Precipitation Products over India for the Peak Southwest Monsoon Season." *International Journal of Climatology* 36: 1614–1631. doi:10.1002/joc.4446.

Prakash, S., A. K. Mitra, E. N. Rajagopal, and D. S. Pai. 2016a. "Assessment of TRMM-based TMPA-3B42 and GSMaP Precipitation Products over India for the Peak Southwest Monsoon Season." *International Journal of Climatology* 36: 1614–1631. doi:10.1002/joc.2016.36.issue-4.

Prakash, S., V. Sathiyamoorthy, C. Mahesh, and R. M. Gairola. 2014. "An Evaluation of High-Resolution Multisatellite Rainfall Products over the Indian Monsoon Region." *International Journal of Remote Sensing* 35: 3018–3035. doi:10.1080/01431161.2014.894661.

Qin, Y., Z. Chen, Y. Shen, S. Zhang, and R. Shi. 2014. "Evaluation Of Satellite Rainfall Estimates over The Chinese Mainland." *Remote Sensing* 6 (11): 11649–11672. doi: 10.3390/rs61111649.

Schneider, U., T. Fuchs, A. Meyer-Christoffer, and B. Rudolf. 2008. "Global Precipitation Analysis Products of the GPCC." *Global Precipitation Climatology Centre DWD: 13*, ftp://ftp.dwd.de/pub/data/gpcc/PDF/GPCC_intro_products_2008.pdf

Sharifi, E., R. Steinacker, and B. Saghafian. 2016. "Assessment of GPM-IMERG and Other Precipitation Products against Gauge Data under Different Topographic and Climatic Conditions in Iran: Preliminary Results." *Remote Sensing* 8: 135. doi:10.3390/rs8020135.

Siuki S. K., B. Saghafian, and S. Moazami. 2017. "Comprehensiveevaluation of 3-Hourly TRMM and Half-Hourly GPM-IMERG Satellite Precipitation Products." *International Journal of Remote Sensing* 38 (2): 558–571. doi:10.1080/01431161.2016.1268735.

Sorooshian, S., K.-L. Hsu, X. Gao, H. V. Gupta, B. Imam, and D. Braithwaite. 2000. "Evaluation of PERSIANN System Satellite-Based Estimates of Tropical Rainfall." *Bulletin of the American Meteorological Society* 81: 2035–2046. doi:10.1175/1520-0477(2000)081<2035:EOPSSE>2.3.CO;2,2.

Sungmin, O., U. Foelsche, G. Kirchengast, J. Fuchsberger, J. Tan, and W. A. Petersen. 2017. "Evaluation of GPM IMERG Early, Late, and Final Rainfall Estimates withWegenerNet Gauge Data in Southeast Austria." *Hydrology Earth System Science Discuss,* 21: 6559-6572. doi:10.5194/hess-2017-256,2017.

Tan, J., W. A. Petersen, and A. Tokay. 2016. "A Novel Approach to Identify Sources of Errors in IMERG for GPM Ground Validation." *Journal of Hydrometeorology* 17: 2477–2491. doi:10.1175/JHM-D-16-0079.1.

Tang, G., Y. Ma, D. Long, L. Zhong, and Y. Hong. 2016. "Evaluation of GPM Day-1 IMERG and TMPA Version-7 Legacy Products over Mainland China at Multiple Spatiotemporal Scales." *Journal of Hydrometeorology* 533: 152–167. doi:10.1016/j.jhydrol.2015.12.008.

Turner, A., and H. Annamalai. 2012. "Climate Change and the South Asian Monsoon." *Nature Climate Change* 2: 587–595. doi:10.1038/nclimate1495.

Ushio, T., K. Sasashige, T. Kubota, S. Shige, K. Okamoto, K. Aonashi, T. Inoue, et al. 2009. "A Kalman Filter Approach to the Global Satellite Mapping of Precipitation (Gsmap) from Combined Passive Microwave and Infrared Radiometric Data". *Journal of the Meteorological Society of Japan* 87: 137–151. doi:10.2151/jmsj.87A.137.

Varma, A. K., and R. M. Gairola. 2015. "Algorithm Theoretical Basis Document: Hydro-Estimator (Modified)". Document No. SAC/EPSA/AOSG/SR/04/2015.

Wang, B., J. Liu, H. J. Kim, P. J. Webster, and S. Y. Kim. 2012. "Recent Change of the Global Monsoon Precipitation (1979–2008)." *Climate Dynamics* 39: 1123–1135. doi:10.1007/s00382-011-1266.z.

Wang, R., J. Chen, and X. Wang. 2017. "Comparison of IMERG Level-3 and TMPA 3B42V7 in Estimating Typhoon-Related Heavy Rain." *Water* 9: 276. doi:10.3390/w9040276.

Webster, P. 2013. "Improve weather forecasts for the developing world." *Nature* 493: 17–19. doi:10.1038/493017a.

Wilks, D. S. 2006. *Statistical Methods in the Atmospheric Sciences*. Second edition.

Xie, P., and P. A. Arkin. 1995. "An Intercomparison of Gauge Observations and Satellite Estimates of Monthly Precipitation." *Journal of Applied Meteorology* 34: 1143–1160. doi:10.1175/1520-0450-(1995)034<1143:AIOGOA>2.0.CO;2.

Yong, B., D. Liu, J. J. Gourley, Y. Tian, G. J. Huffman, L. Ren, and Y. Hong. 2015. "Global View of Real-Time TRMM Multisatellite Precipitation Analysis: Implications for Its Successor Global Precipitation Measurement Mission." *Bulletin of the American Meteorological Society* 96: 283–296. doi:10.1175/BAMS-D-14-00017.1.